


**Squeezed-state evolution and entanglement in lossy coupled-resonator optical waveguides**

Hossein Seifoory\* and Marc M. Dignam

*Department of Physics, Engineering Physics and Astronomy, Queen's University, Kingston, Ontario K7L 3N6, Canada* (Received 23 October 2017; published 26 February 2018)

We investigate theoretically the temporal evolution of a squeezed state in lossy coupled-cavity systems. We present a general formalism based upon the tight-binding approximation and apply this to a two-cavity system as well as to a coupled-resonator optical waveguide in a photonic crystal. We derive analytical expressions for the number of photons and the quadrature noise in each cavity as a function of time when the initial excited state is a squeezed state in one of the cavities. We also analytically evaluate the time-dependent cross correlation between the photons in different cavities to evaluate the degree of quantum entanglement. We demonstrate that loss in such coupled-cavity systems cannot be treated using simple exponential factors. Finally, we also derive approximate analytic expressions for the maximum photon number, maximum squeezing, and maximum entanglement for cavities far from the initially excited cavity in a lossless coupled-resonator optical waveguide.

DOI: [10.1103/PhysRevA.97.023840](https://doi.org/10.1103/PhysRevA.97.023840)**I. INTRODUCTION**

Nonclassical states of light possess properties that can only be described by quantum theory. One potential attribute of these states is quantum entanglement, which has potential applications in quantum teleportation, quantum computation, and quantum information [1,2]. Both discrete variables (DVs) and continuous variables (CVs) can be used to create quantum entanglement between two distant quantum systems. However, implementation of DV entanglement currently suffers from difficulties in single-photon generation and detection and from loss in integrated on-chip systems. In contrast, CV entanglement as an alternative to its DV counterpart can be efficiently created and used for implementation of CV quantum protocols [3–7] and has the advantage that the entanglement is generally more robust to loss than systems composed of photon pairs.

Generally, nonuniformly distributed quadrature fluctuations of squeezed light can provide CV entanglement [8,9]. The inseparability criterion, which is based on the total variance of a pair of canonical conjugates variables, can be used to study the degree of quantum correlation in CV systems [10,11]. Although the CV entangled light has been achieved using bulk setups [6,8,12–14], the migration from bulk optics to integrated photonics seems inevitable since, as the size and complexity of these systems increase, the limitations of working with bulk optics, such as stability, precision, and physical size, become significant. Due to recent developments in integrated photonics technology, it is possible to resolve scalability and stability concerns associated with bulk optics by generating CV entanglement on a chip [15]. However, the effects of environmental loss, which destroys the nonclassical properties of light and consequently affects the entanglement [16], are inevitable and need to be understood and managed.

Parametric down conversion (PDC), in which a pump photon is annihilated to produce a signal and an idler photon, is one

of the processes that can be used to generate correlated photons [17–19]. It has been shown that photon pairs can be generated via PDC in integrated on-chip systems using nonlinear materials with high susceptibility, such as AlGaAs [20]. Thanks to the maturity achieved in fabrication technology and the ability to integrate them with other photonic elements, propagation in nonlinear waveguides is now a very promising way in which to generate entangled photon states via PDC [21,22]. The pumping can be done either from one end of the waveguide or from the top. However, the latter configuration is more interesting for two key reasons. First, by focusing the pump light from above on a single-resonant cavity, one can achieve a high intensity of pump light in the nonlinear material, which increases the generation rate. Second, it enables the generation of entangled photons at two distant locations, which is desired in many quantum communications applications. Such a source of counterpropagating twin photons has been experimentally demonstrated in an AlGaAs ridge waveguide [21,22]. This same configuration of top pumping of a nonlinear waveguide is also very promising for creating entangled squeezed states. It is this system that we examine in this paper. The particular system that we will consider is the coupled-resonator optical waveguide (CROW).

CROWs, which were first studied by Yariv *et al.* [23], can be described as a waveguide consisting of weakly-coupled optical cavities along one dimension. The tight-binding method [24,25], which uses localized single-cavity modes as a basis, can be applied as a mathematical framework to model the evolution of light in such a coupled structure. One nice feature of CROWs is that by adjusting the nature of the cavities and the separation between the cavities, one can adjust the dispersion and even the loss to some degree to optimize the system for a particular application [23]. This characteristic is the main advantage of using CROWs compared to conventional optical waveguides, in which the guiding properties are mostly determined by total internal reflection and material dispersion. An intrinsic property of CROWs, however, is scattering loss; this must therefore be included in any treatment of these systems. As we shall show, the effects of loss on the

\*hossein.seifoory@queensu.ca

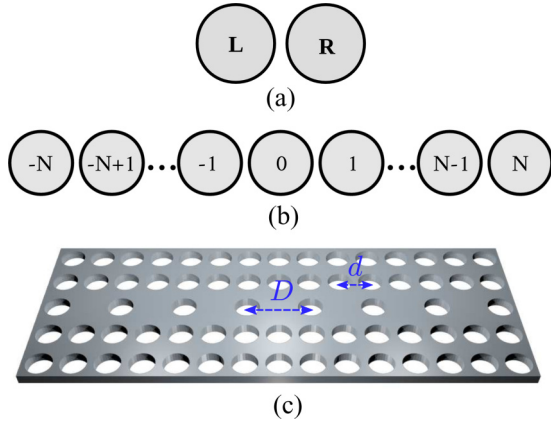


FIG. 1. Schematic picture of (a) two coupled cavities, (b) a CROW structure, and (c) the particular CROW structure with period  $D$  formed from defects in a slab photonic crystal with a square lattice of period  $d$ .

quantum correlations in these systems are nontrivial and cannot generally be treated using a simple exponential factor.

In our previous work, we studied the generation of a squeezed vacuum state (SVS) in the presence of loss and showed how the loss affects the generation of squeezed light [26]. Now we are interested in the evolution and propagation of squeezing and entanglement in lossy systems. In this work, we develop a general formalism to study the squeezing and the entanglement in lossy coupled-cavity structures and apply it to a CROW structure. The CROW is interesting because it has been shown to have potential in generating CV entangled states between two spatially separated sites [27] and can also be integrated with other photonic components, such as side cavities [28,29], forming an integrated photonic circuit, for use in photonic quantum information processing.

In this paper, we show that the time evolution of the quadrature variances and the number of photons in each cavity can be explained and parametrized using a tight-binding approach. This method allows us to calculate the CV correlation variance between the photons in different cavities. The full analytic study of the squeezed state evolution in a lossy coupled-cavity system can provide us with insight into the influence of coupling and loss on the photon statistics and the nonclassical properties of the photons inside each cavity. We present the analytic expressions for a general initial state, but only explicitly present detailed results for an initial state which is a squeezed vacuum state in one of the cavities.

The paper is organized as follows. In Sec. II, we present the tight-binding formalism that is used to obtain the quasimodes [30] of the coupled-cavity system. We then derive the time-dependent equations for the number of photons, the quadrature noise, and the CV correlation variance in a lossy coupled-cavity system with a general initial state. In Sec. III, as a test system, we study the state evolution in a lossy two-coupled-cavity system [see Fig. 1(a)], where the initial state is a squeezed state in one of the cavities. In Sec. IV, we apply our approach to examine the same quantities for the state in the more technologically interesting CROW structure [see Figs. 1(b) and 1(c)], where the initial state is also a squeezed state in one of the cavities. Finally, in Sec. V, we present our conclusions.

## II. GENERAL FORMALISM

In this section, we first present the general form of tight-binding theory and derive the general expressions for some important quantities such as the time evolution of photon number, variances of quadrature operators, and correlation variance in lossy coupled-cavity systems.

Although in this paper we mainly focus on SVS as the initial state of the  $c$ th cavity, in this section we consider a more general case and present analytic results for a general initial state.

Using the tight-binding formalism [25,31], we can determine the fields and complex frequencies for the leaky modes of a coupled-cavity system. This formalism allows us to determine the mode fields and frequencies of a lossy coupled-cavity structure using only one finite-difference time-domain (FDTD) calculation.

The modes of a system can be obtained by solving the corresponding homogeneous Helmholtz equation for the electric field. However, here, due to the leakage in the system, we employ *quasimodes* (QMs) which are electromagnetic resonances of an open (leaky) dielectric structure and are characterized by complex frequencies,  $\tilde{\omega}_m$ . We denote the complex mode field of these QMs by  $\tilde{\mathbf{N}}_m(\mathbf{r})$ .

Following Fussel and Dignam [25], we begin by expanding the coupled-cavity QMs,  $\tilde{\mathbf{N}}_m(\mathbf{r})$ , in terms of single-cavity QMs,  $\tilde{\mathbf{M}}_q(\mathbf{r})$ , as

$$\tilde{\mathbf{N}}_m(\mathbf{r}) = \sum_q v_{mq} \tilde{\mathbf{M}}_q(\mathbf{r}), \quad (1)$$

where  $q$  labels the mode associated with a given cavity,  $m$  labels a given coupled-cavity mode, and  $v_{mq}$  are the expansion coefficients. The quasimodes are the solutions to the homogeneous Helmholtz equation for the electric field in the coupled-cavity and single-cavity structures:

$$\nabla \times \nabla \times \tilde{\mathbf{N}}_m(\mathbf{r}) - \frac{\tilde{\omega}_m^2}{c^2} \epsilon(\mathbf{r}) \tilde{\mathbf{N}}_m(\mathbf{r}) = 0, \quad (2)$$

$$\nabla \times \nabla \times \tilde{\mathbf{M}}_q(\mathbf{r}) - \frac{\tilde{\Omega}_q^2}{c^2} \epsilon_q(\mathbf{r}) \tilde{\mathbf{M}}_q(\mathbf{r}) = 0, \quad (3)$$

where  $\tilde{\omega}_m \equiv \omega_m - i\gamma_m$  is the complex frequency for the  $m$ th QM of the coupled-cavity structure and  $\tilde{\Omega}_q \equiv \Omega_q - i\Gamma_q$  is the complex frequency of the  $q$ th cavity. Also,  $\epsilon(\mathbf{r})$  and  $\epsilon_q(\mathbf{r})$  are the dielectric material profiles of the full coupled-cavity structure and the structure that only contains the  $q$ th cavity, respectively. The single-cavity modes and frequencies are calculated using FDTD.

Substituting Eq. (1) into Eq. (2) and then using Eq. (3) leads to the generalized eigenvalue equation,

$$\tilde{\mathbf{A}} \tilde{\Omega} \tilde{\mathbf{v}} = \tilde{\Lambda} (\tilde{\mathbf{A}} + \tilde{\mathbf{B}}) \tilde{\mathbf{v}}, \quad (4)$$

where  $\tilde{\Lambda} \equiv \text{Diag}\{\tilde{\omega}_m^2\}$ ,  $\tilde{\Omega} \equiv \text{Diag}\{\tilde{\Omega}_q^2\}$ , and  $\tilde{\mathbf{v}} \equiv \{v_{mq}\}$ , and  $\tilde{\mathbf{A}}$  and  $\tilde{\mathbf{B}}$  are, respectively, the overlap and coupling coefficients between the  $p$ th and  $q$ th cavities, with elements defined as

$$\tilde{A}_{qp} = \int d^3\mathbf{r} \epsilon_q(\mathbf{r}) \tilde{\mathbf{M}}_q^*(\mathbf{r}) \cdot \tilde{\mathbf{M}}_p(\mathbf{r}), \quad (5)$$

$$\tilde{B}_{qp} = \int d^3\mathbf{r} \delta\epsilon_q(\mathbf{r}) \tilde{\mathbf{M}}_q^*(\mathbf{r}) \cdot \tilde{\mathbf{M}}_p(\mathbf{r}), \quad (6)$$

where  $\delta\epsilon_q(\mathbf{r}) \equiv \epsilon(\mathbf{r}) - \epsilon_q(\mathbf{r})$ .

Using the expansion coefficients  $v_{mq}$ , the annihilation operator  $b_m$ , for the  $m$ th mode of the coupled-cavity system, can be written in terms of the  $q$ th individual single-mode cavity operators  $a_q$  as

$$b_m = \sum_q \tilde{v}_{mq}^* a_q. \quad (7)$$

Although we will be interested in the nature of the states in individual cavities, the evolution is most simply calculated using the full coupled-cavity annihilation operators. This evolution is found by solving the adjoint master equation for this open, lossy system [32]. We have previously shown that for any product of normally-ordered operators, the time dependence of the individual annihilation operators is given by

$$b_m(t) = b_m e^{-i\tilde{\omega}_m t}, \quad (8)$$

where  $b_m = b_m(0)$  is the corresponding operator in the Schrödinger representation [33] and the time evolution of the creation operator is simply the Hermitian conjugate of Eq. (8).

Using Eqs. (7) and (8), one can generally write the time-dependent localized field operator in a coupled-cavity system in terms of expansion coefficients and the operators at  $t = 0$  as

$$a_p(t) = \sum_{mq} \tilde{v}_{mq}^* a_q e^{-i\tilde{\omega}_m t} \tilde{v}_{mp}. \quad (9)$$

Using Eq. (9) and its complex conjugate, the time-dependent average photon number in the  $p$ th cavity can be written as

$$\langle a_p^\dagger(t) a_p(t) \rangle = \sum_{mqm'q'} \langle a_q^\dagger a_{q'} \rangle \tilde{v}_{mp}^* \tilde{v}_{mq} \tilde{v}_{m'q'}^* \tilde{v}_{m'p} e^{-i(\tilde{\omega}_{m'} - \tilde{\omega}_m^*)t}. \quad (10)$$

Following the same procedure for the quadrature operators,  $X_p = a_p + a_p^\dagger$  and  $Y_p = i(a_p - a_p^\dagger)$ , the time-dependent variances of  $X$  quadrature operator in general form can be shown to be

$$\begin{aligned} \langle (\Delta X_p)^2 \rangle &= 1 + \sum_{mqm'q'} (2 \langle a_q^\dagger a_{q'} \rangle \tilde{v}_{mp}^* \tilde{v}_{mq} \tilde{v}_{m'q'}^* \tilde{v}_{m'p} e^{-i(\tilde{\omega}_{m'} - \tilde{\omega}_m^*)t} \\ &+ \langle a_q a_{q'} \rangle \tilde{v}_{mp}^* \tilde{v}_{mq} \tilde{v}_{m'q'}^* \tilde{v}_{m'p} e^{-i(\tilde{\omega}_{m'} + \tilde{\omega}_m)t} \\ &+ \langle a_q^\dagger a_{q'}^\dagger \rangle \tilde{v}_{mp}^* \tilde{v}_{mq} \tilde{v}_{m'q'}^* \tilde{v}_{m'p} e^{i(\tilde{\omega}_{m'} + \tilde{\omega}_m^*)t}). \end{aligned} \quad (11)$$

To obtain the general form of  $\langle (\Delta Y_p)^2 \rangle$ , one just needs to change the sign of the last two terms in Eq. (11), containing  $\langle a_q a_{q'} \rangle$  and  $\langle a_q^\dagger a_{q'}^\dagger \rangle$ .

We now study the degree of entanglement between the photons in cavities  $p$  and  $p'$  in a coupled-cavity structure using correlation variance, which is defined as [10,11]

$$\Delta_{p,p'}^2 = \langle [\Delta(X_p - X_{p'})]^2 \rangle + \langle [\Delta(Y_p + Y_{p'})]^2 \rangle. \quad (12)$$

Employing Eq. (9) and its complex conjugate in Eq. (12), the general form of the time-dependent correlation variance can be written as

$$\begin{aligned} \Delta_{p,p'}^2 &= 4 + 4 \sum_{mqm'q'} [\langle a_q^\dagger a_{q'} \rangle (\tilde{v}_{mp}^* \tilde{v}_{mq} \tilde{v}_{m'q'}^* \tilde{v}_{m'p} \\ &+ \tilde{v}_{mp}^* \tilde{v}_{mq} \tilde{v}_{m'q'}^* \tilde{v}_{m'p}) e^{-i(\tilde{\omega}_{m'} - \tilde{\omega}_m^*)t}] \end{aligned}$$

$$\begin{aligned} &- 4 \sum_{mqm'q'} \langle a_q a_{q'} \rangle \tilde{v}_{mp}^* \tilde{v}_{mq} \tilde{v}_{m'q'}^* \tilde{v}_{m'p} e^{-i(\tilde{\omega}_{m'} + \tilde{\omega}_m)t} \\ &- 4 \sum_{mqm'q'} \langle a_q^\dagger a_{q'}^\dagger \rangle \tilde{v}_{mp}^* \tilde{v}_{mq} \tilde{v}_{m'q'}^* \tilde{v}_{m'p} e^{i(\tilde{\omega}_{m'} + \tilde{\omega}_m^*)t}. \end{aligned} \quad (13)$$

Equations (10), (11), and (13) give the results for general initial conditions. In the rest of this paper, we assume that at time  $t = 0$ , the  $c$ th cavity is in an excited state of light and the rest of the cavities are in the vacuum state; thus, in what follows, the only nonvanishing terms in Eqs. (10), (11), and (13) are those in which  $q = q' = c$ . Before proceeding, we first briefly review some of the quantum properties of different initial states in a single cavity. In Table I, we summarize some properties of three different initial states: the SVS, squeezed thermal state (STS), and coherent state. In Table I,  $\tilde{\eta}$  is the coherent state parameter, and  $n_{th}$  is the thermal photon number for the STS. For the SVS and STS, the squeezing parameter is generally complex and we write it in the form  $\xi = u e^{i\phi}$ , where  $u$  and  $\phi$  are the squeezing amplitude and phase, respectively.

The formalism introduced here is used in the following sections to study the temporal evolution of a SVS, first in a simple two-coupled-cavity system and then in a CROW structure. Before moving to the next section, it is worth mentioning that although there are several different methods that can be used to model coupled optical systems [16,34], our method, unlike many of the other methods, provides analytic solutions that are independent of the number of coupled cavities and so can be easily used to treat photons in CROW systems. In addition, unlike previous approaches used to treat nonclassical states of light in similar structures [16,35], our method includes an exact treatment of intrinsic scattering in systems in which there are losses that are mode dependent.

### III. TWO LOSSY COUPLED CAVITIES

We first consider a system consisting of only two identical lossy coupled cavities, shown in Fig. 1(a). This system supports two QMs,  $\tilde{\omega}_+$  and  $\tilde{\omega}_-$ , representing the symmetric and antisymmetric QMs, respectively. It has been shown that in the nearest-neighbor tight-binding (NNTB) approximation, the complex frequencies of the QMs of a two-coupled-cavity system can be written in terms of coupling parameters [36,37] as

$$\tilde{\omega}_\pm \simeq \tilde{\Omega}_0 (1 \pm \tilde{\beta}_1/2), \quad (14)$$

TABLE I. The operator expectation values for the SVS, STS, and coherent state for the  $c$ th cavity at  $t = 0$ . Here,  $u$  and  $\phi$  are the squeezing amplitude and phase, respectively, for the SVS and STS,  $\tilde{\eta}$  is the coherent state parameter, and  $n_{th}$  is the thermal photon number for the STS.

	SVS	STS	Coherent state
$\langle a_c^\dagger a_c \rangle$	$\sinh^2(u)$	$n_{th} \cosh(2u) + \sinh^2(u)$	$ \tilde{\eta} ^2$
$\langle a_c a_c \rangle$	$-e^{i\phi} \cosh(u) \sinh(u)$	$-(n_{th} + \frac{1}{2}) e^{i\phi} \sinh(2u)$	$\tilde{\eta}^2$
$\langle a_c^\dagger a_c^\dagger \rangle$	$-e^{-i\phi} \cosh(u) \sinh(u)$	$-(n_{th} + \frac{1}{2}) e^{-i\phi} \sinh(2u)$	$\tilde{\eta}^{*2}$

where  $\tilde{\beta}_1 \equiv \tilde{B}_{LR}$ . The general quantum states of such a system can be expanded in terms of the two individual cavity states as

$$\tilde{\mathbf{M}}_{\pm}(\mathbf{r}) = \frac{1}{\sqrt{2}}[\tilde{\mathbf{N}}_L(\mathbf{r}) \pm \tilde{\mathbf{N}}_R(\mathbf{r})], \quad (15)$$

where  $\tilde{\mathbf{N}}_L(\mathbf{r})$  and  $\tilde{\mathbf{N}}_R(\mathbf{r})$  are the modes of the left and right cavities, respectively. Using Eq. (7) with  $v_{+L} = v_{+R} = 1/\sqrt{2}$  and  $v_{-L} = -v_{-R} = 1/\sqrt{2}$ , one can also write the coupled-cavity operators as symmetric and antisymmetric superpositions of the localized site operators as

$$b_+ = \frac{1}{\sqrt{2}}(a_L + a_R) \quad (16)$$

and

$$b_- = \frac{1}{\sqrt{2}}(a_L - a_R), \quad (17)$$

where  $a_L$  and  $a_R$  are the annihilation operators acting on the left and right cavities, respectively.

To examine the propagation and time evolution of nonclassical light in lossy coupled-cavity structures, we begin by studying the evolution of squeezed light in our lossy two-cavity system. Using Eqs. (10), (11), and (13), we study the time evolution of the quadrature variances and photon statistic of states in both cavities to investigate whether the light transferred to the second cavity maintains its nonclassical properties and to determine the correlations between light in the different cavities.

In all the following equations, the specific state of the  $c$ th cavity at  $t = 0$  is general. Table I can be used to obtain results for specific initial states. However, all plotted results in this section will be for the initial state where the  $c$ th cavity is the left cavity, which is in a SVS with  $u = 1.2$  and  $\phi = 0$ . We set  $\tilde{\omega}_{\pm} = \omega_{\pm} - i\gamma_{\pm}$  and, for simplicity, we assume that  $\gamma_+ = \gamma_- = \gamma$  and define  $\omega_+ = \omega$  and  $\omega_+ - \omega_- = \Delta$ . We choose  $\Delta = \omega/20$  and  $\gamma = 0.02\Delta$ . The parameters are chosen to demonstrate some of the key features, which are the beating back and forth between the two cavities, the free oscillations, and the loss in the system.

Using Eq. (10), the time-dependent average number of photons in the cavities can then be written as

$$\langle a_R^\dagger(t)a_R(t) \rangle = \frac{1}{4} \langle a_L^\dagger a_L \rangle (e^{i(\tilde{\omega}_+^* - \tilde{\omega}_+)t} - e^{i(\tilde{\omega}_+^* - \tilde{\omega}_-)t} - e^{i(\tilde{\omega}_-^* - \tilde{\omega}_+)t} + e^{i(\tilde{\omega}_-^* - \tilde{\omega}_-)t}), \quad (18)$$

$$\langle a_L^\dagger(t)a_L(t) \rangle = \frac{1}{4} \langle a_L^\dagger a_L \rangle (e^{i(\tilde{\omega}_+^* - \tilde{\omega}_+)t} + e^{i(\tilde{\omega}_+^* - \tilde{\omega}_-)t} + e^{i(\tilde{\omega}_-^* - \tilde{\omega}_+)t} + e^{i(\tilde{\omega}_-^* - \tilde{\omega}_-)t}), \quad (19)$$

which can be simplified as

$$\langle a_R^\dagger(t)a_R(t) \rangle = \frac{1}{2} \langle a_L^\dagger a_L \rangle e^{-2\gamma t} [1 - \cos(\Delta t)] \quad (20)$$

and

$$\langle a_L^\dagger(t)a_L(t) \rangle = \frac{1}{2} \langle a_L^\dagger a_L \rangle e^{-2\gamma t} [1 + \cos(\Delta t)]. \quad (21)$$

As expected, for lossy systems, the number of photons in both cavities decays to zero at long times due to the exponential decay coefficient in Eqs. (20) and (21).

Following the same procedure as before and using Eq. (11), the variances of quadrature operators can be shown to be

$$\begin{aligned} \langle \Delta X^2 \rangle_{(L,R)} &= 1 + e^{-2\gamma t} [1 \pm \cos(\Delta t)] (\langle a_L^\dagger a_L \rangle \\ &\quad \pm \frac{1}{2} \langle a_L a_L \rangle e^{-i(2\omega - \Delta)t} \\ &\quad \pm \frac{1}{2} \langle a_L^\dagger a_L^\dagger \rangle e^{i(2\omega - \Delta)t}) \end{aligned} \quad (22)$$

and

$$\begin{aligned} \langle \Delta Y^2 \rangle_{(L,R)} &= 1 + e^{-2\gamma t} [1 \pm \cos(\Delta t)] (\langle a_L^\dagger a_L \rangle \\ &\quad \mp \frac{1}{2} \langle a_L a_L \rangle e^{-i(2\omega - \Delta)t} \\ &\quad \mp \frac{1}{2} \langle a_L^\dagger a_L^\dagger \rangle e^{i(2\omega - \Delta)t}), \end{aligned} \quad (23)$$

where the upper (lower) signs belong to the left (right) cavity. In Fig. 2(a), we plot the mean photon number in each cavity as it evolves in time for a SVS. As can be seen, the photons, which are all initially in the left cavity, periodically move in time between the two cavities. It is also evident that the mean photon number gradually decreases due to the scattering loss. The time-dependent quadrature noise in  $X$  is shown in Figs. 2(b) and 2(c) for the left and right cavity, respectively. The dashed lines indicate the classical limit, below which the quadrature noise is squeezed. As expected, the quadrature noise in the left cavity is initially less than this limit ( $\langle \Delta X(t=0) \rangle_L = 0.3$ ) since it is a SVS. On the other hand, the right cavity at  $t = 0$  is vacuum and consequently has the minimum classical quadrature noise,  $\Delta X_R = 1$ . As the coupled system evolves in time, we can see that the  $\Delta X_R$  falls below the classical limit and reaches 0.4 at  $\Delta t = \pi$ , which confirms that the squeezed state has been transferred to the right cavity due to the coupling between the two cavities. In the absence of loss, this squeezing would be identical to the squeezing in the left cavity at  $t = 0$ .

Before moving to the CROW structure, we evaluate the entanglement between the light in these two cavities. It has been shown that  $\Delta_{L,R}^2 < 4$  can be considered as the inseparability criterion for entanglement [10, 11, 15, 38]. Using Eq. (13) and considering the same initial condition as before, the time-dependent correlation variance is found to be

$$\begin{aligned} \Delta_{L,R}^2 &= 4 + e^{-2\gamma t} [4 \langle a_L^\dagger a_L \rangle \\ &\quad - \langle a_L a_L \rangle e^{i\Delta t} (e^{-i(2\omega + \Delta)t} - e^{-i(2\omega - \Delta)t}) \\ &\quad - \langle a_L^\dagger a_L^\dagger \rangle e^{-i\Delta t} (e^{+i(2\omega + \Delta)t} - e^{+i(2\omega - \Delta)t})]. \end{aligned} \quad (24)$$

Using Eq. (24) for a lossless system and considering the initial excited state in the left cavity to be a SVS with large squeezing amplitude ( $u \gg 1$ ), it can be shown that the minimum achievable value of  $\Delta_{L,R}^2$  is 2, which is well below the inseparability limit. In Fig. 2(d), we plot the CV correlation variance as a function of time. As can be seen, the correlation variance exceeds the inseparability criterion reaching local minima close to the times  $\Delta t = (2l + 1)\pi/2$ , where  $l$  is an integer. As expected, the loss affects the degree of inseparability as the system evolves in time. For instance, due to loss, although the correlation variance at  $\Delta t = 7\pi/2$  is still below the inseparability limit, it experiences about a 22% increase compared to the time  $\Delta t = \pi/2$  where  $\Delta_{L,R}^2 \approx 2.3$ .

Before moving to the next section, we note that in this two-cavity system, because in the numerical results that we plotted, we have made a simplifying assumption that the loss in the two modes is identical the decay takes the form of a simple

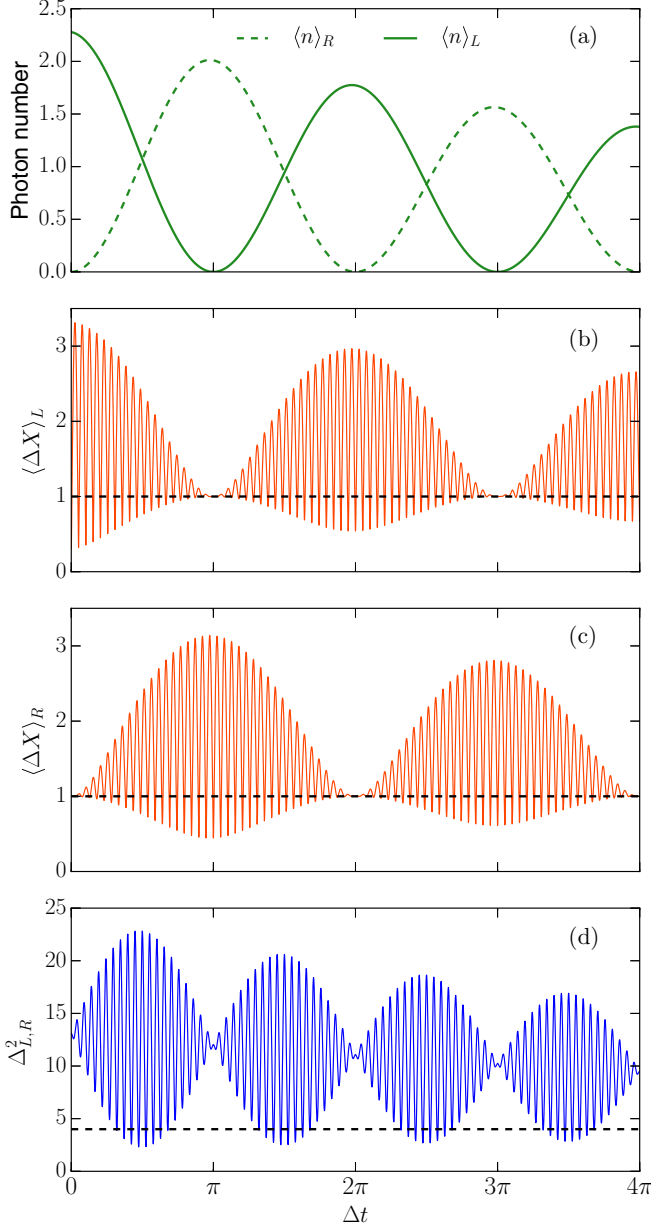


FIG. 2. Calculated results for the two-coupled-cavity system. (a) Time evolution of the mean photon number in the left (solid line) and right (dashed line) cavities. The time evolution of the quadrature noise in  $X$  in (b) the left and (c) the right cavities. The dashed line at  $\langle \Delta X \rangle_{(L,R)} = 1$  shows the classical limit for the quadrature noises. (d) The CV correlation variance as a function of time. The dashed line in (d) shows the inseparability limit below which the light is considered to be entangled.

exponential. However, if we had not made that assumption, the loss behavior would become more complicated; we will see such effects in the next section where we study the evolution in a CROW structure.

#### IV. COUPLED-RESONATOR OPTICAL WAVEGUIDES

Although the simple two-coupled-cavity system is a useful test bench for understanding the evolution of different states of light in lossy coupled systems, to be more practical, we

examine a CROW structure, in which the light can propagate over a longer distance. Such a system, consisting of  $2N + 1$  weakly-coupled, lossy optical cavities along one dimension with a periodicity  $D$ , is schematically shown in Fig. 1(b). As discussed in Sec. II, this system can be studied using the tight-binding method which assumes weak coupling between different cavities and uses a localized single-mode cavity as a basis.

Assuming that all the cavities are identical and support the same mode with complex frequency,  $\tilde{\Omega}_p = \tilde{\Omega}_0$ , and using the fact that  $\tilde{A}_{pq} = \tilde{A}_{p-q}$  and  $\tilde{B}_{pq} = \tilde{B}_{p-q}$  in Eq. (4), then applying periodic boundary condition and Bloch's theorem, the tight-binding dispersion can be written as

$$\tilde{\omega}(k) = \tilde{\Omega}_0 \sqrt{\frac{1 + 2 \sum_{p=1}^N \cos(kpD) \tilde{\alpha}_p}{1 + 2 \sum_{p=1}^N \cos(kpD) (\tilde{\alpha}_p + \tilde{\beta}_p)}}, \quad (25)$$

where  $\tilde{\alpha}_p \equiv \tilde{A}_{0p}$  and  $\tilde{\beta}_p \equiv \tilde{B}_{0p}$ . Using the NNTB approximation, where only  $\tilde{\beta}_1 \neq 0$  in Eq. (25), we obtain

$$\tilde{\omega}(k) \approx \tilde{\Omega}_0 [1 - \tilde{\beta}_1 \cos(kD)], \quad (26)$$

where we used the Taylor expansion of the square-root function. It can be seen from Eq. (26) that the modes of the CROW experience different loss rates, which can differ by an order of magnitude [39,40]. Again from NNTB, we obtain

$$v_{kp} = \frac{e^{ikpD}}{\sqrt{N}}. \quad (27)$$

We take the  $c$ th cavity to be initially in a squeezed vacuum state, while all other cavities are in the vacuum state. Such a state could be achieved, for example, by strongly pumping the  $c$ th cavity in the presence of spontaneous parametric down-conversion [41,42], as long as the pump duration is much shorter than the time required for transfer to the neighboring cavities.

Employing Eqs. (10) and (27), the time-dependent average photon number in the  $p$ th cavity can be written as

$$\langle a_p^\dagger(t) a_p(t) \rangle = \frac{1}{N^2} \sum_{kqk'q'} \langle a_q^\dagger a_{q'} \rangle (e^{-ik(p-q)D} e^{ik'(p-q')D} \times e^{-i\tilde{\Omega}_0[1-\tilde{\beta}_1^* \cos(kD)]t} e^{-i\tilde{\Omega}_0[1-\tilde{\beta}_1 \cos(k'D)]t}). \quad (28)$$

For our initial conditions, the only nonvanishing expectation value in Eq. (28) is  $\langle a_c^\dagger a_c \rangle = \sinh^2(u)$ . Converting the sums to integrals and using the following equations:

$$\int_0^\pi \cos[\tilde{z} \cos(x)] \cos(nx) dx = \pi \cos\left(\frac{n\pi}{2}\right) J_n(\tilde{z}), \quad (29a)$$

$$\int_0^\pi \sin[\tilde{z} \cos(x)] \cos(nx) dx = \pi \sin\left(\frac{n\pi}{2}\right) J_n(\tilde{z}), \quad (29b)$$

where  $n$  is an integer and  $J_n(\tilde{z})$  is the Bessel function of the first kind of order  $n$  [43], one finds that the time-dependent average photon number in the  $p$ th cavity is

$$\langle a_p^\dagger(t) a_p(t) \rangle = \langle a_c^\dagger a_c \rangle e^{-2\gamma t} |\mathcal{J}_{\delta p}(\tilde{\zeta}_1 t)|^2, \quad (30)$$

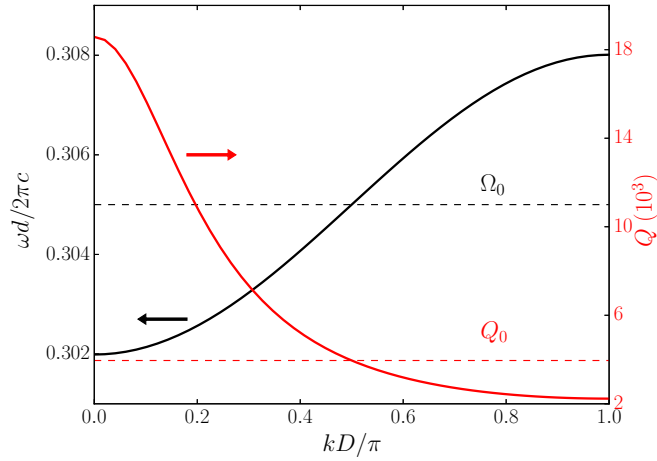


FIG. 3. Frequency (left axis) and quality factor (right axis) as a function of the Bloch vector for the CROW structure. The dashed black and red lines represent the resonant frequency and the quality factor for the individual cavity, respectively.

where  $\tilde{\zeta}_1 \equiv \tilde{\Omega}_0 \tilde{\beta}_1$ ,  $\gamma = -\text{Im}(\tilde{\Omega}_0)$ , and  $\delta p \equiv p - c$ . To scale the time, we define  $\tau = 1/\text{Re}\tilde{\zeta}_1$ , which is the minimum time for a pulse to travel one period. In all of the plots in this section, it is assumed that the  $c$ th cavity is the one in the middle of the CROW structure ( $c = 0$ ) and it contains a SVS with  $u = 0.88$  and  $\phi = 0$ , while the rest are initially in the vacuum state.

The physical parameters of the CROW considered in this paper are from Ref. [25]. The CROW consists of a dielectric slab of refractive index  $n = 3.4$  having a square array of cylindrical air void of radius  $a = 0.4d$ , height  $h = 0.8d$ , and lattice vectors  $\mathbf{a}_1 = d\hat{\mathbf{x}}$  and  $\mathbf{a}_2 = d\hat{\mathbf{y}}$ , where  $d$  is the period. The cavities are point defects formed by periodically removing air voids in a line with  $D = 2d$  [see Fig. 1(c)]. The complex frequency  $\tilde{\Omega}_0$  and the complex coupling parameter  $\tilde{\beta}_1$  of the structure are  $(0.305 - i7.71 \times 10^{-5})4\pi c/D$  and  $9.87 \times 10^{-3} - i1.97 \times 10^{-4}$ , respectively.

In Fig. 3, we plot the mode frequency and quality factor as a function of the Bloch vector for our CROW structure. As can be seen, the group velocity and quality factor of the modes differ greatly across the first Brillouin zone. In particular, the group velocity (slope of the frequency plot) is zero at the zone center and at the zone edges. In addition, the quality factor of the modes at the zone center is 8.3 times larger than for the modes at the zone edges. This wide variation in the loss of the different modes has a significant effect on the loss dynamics in the system, as we shall see.

In Fig. 4, we plot the number of photons in the  $p$ th cavity for  $p = 0, 2, 4, 6$  as a function of time for both lossy (solid green line) and lossless (dashed gray line) systems. As can be seen, the number of photons in each cavity decreases as the system evolves in time. However, in addition to the cavity leakage into the environment, coupling between the cavities also affects the number of photons in each cavity. In other words, even in the lossless system (dashed gray line), we still see in Fig. 4 that due to the multiple photon hopping back and forth between the cavities, the maximum number of photons in the  $p$ th cavity gets smaller as  $p$  gets larger. The propagation of light between the coupled cavities is evident in Figs. 4(b)–4(d). As can be seen,

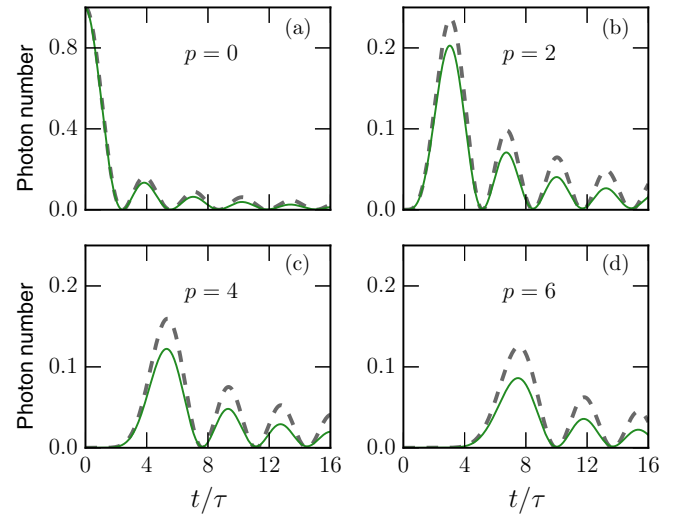


FIG. 4. Average photon number in the (a) central, (b) second, (c) fourth, and (d) sixth cavities as a function of time for the CROW structure. The dashed gray lines show the cases in which the effects of loss are ignored. Note the different scaling in (a).

as the cavity index increases from  $p = 2$  to  $p = 6$ , a longer time is needed for the photons to travel from the  $c$ th cavity to the  $p$ th. If we consider a lossless system, then what one needs to calculate the time at which the photon number in each cavity reaches the maximum value is to find the first maximum of the Bessel function. From Ref. [44], it can be shown that for the cavities far from the  $c$ th cavity (large  $p$ ), the first maximum occurs at the time

$$\frac{t_p}{\tau} \approx p + c_0 p^{1/3}, \quad (31)$$

where  $c_0 \approx 0.8$ . Using Eqs. (26) and (30), the effective propagation velocity (defined as the distance to the cavity divided by the time required to reach the cavity) is then given approximately by

$$v_p = \frac{pD}{t_p} \approx v_{\max}(1 - c_0 p^{-2/3}), \quad (32)$$

where  $v_{\max} = D/\tau$  is the maximum group velocity, which is about 0.04 of the speed of light in vacuum for this CROW structure.

Summing the average number of photons in each cavity and applying Neumann's addition theorem [43], the total number of photons in the system at time  $t$  is given by

$$N_{\text{tot}} = \sum_p \langle a_p^\dagger(t) a_p(t) \rangle = \langle a_c^\dagger a_c \rangle e^{-2\gamma t} I_0(2\text{Im}(\tilde{\zeta}_1 t)), \quad (33)$$

where  $I_0$  is the zeroth-order modified Bessel function of the first kind. Ignoring the losses in the system, it can be shown that the total number of photons in the system is simply  $\sinh^2(u)$  for all  $t$ , which is exactly the number of photons in the  $c$ th cavity at time  $t = 0$ . Also, note that although  $I_0(2\text{Im}(\tilde{\zeta}_1 t))$  monotonically increases with time, the total number of photons still decreases as the system evolves in time due to the dominant exponential factor  $e^{-2\gamma t}$  in Eq. (33). Using a series expansion of the Bessel function, it can be shown that for the time range considered in this paper, the total number of photons in the

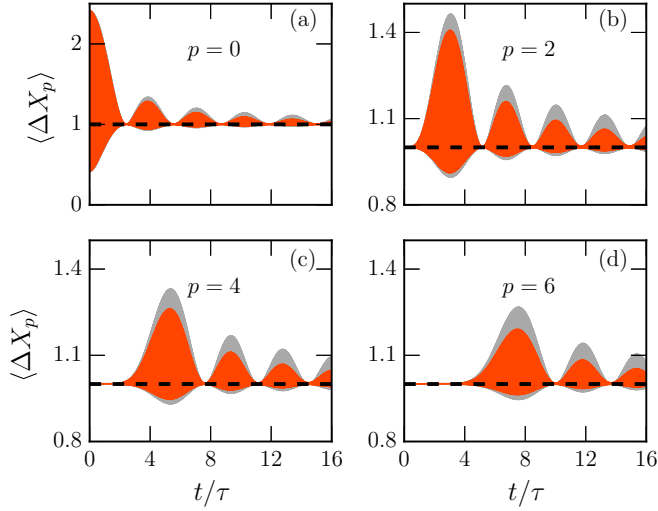


FIG. 5. Quadrature noise in  $X$  in the (a) central, (b) second, (c) fourth, and (d) sixth cavities as a function of time for the CROW. The deviation from a lossless system, shown with light gray, is evident in each case. Note the different scaling in (a) and note that there are fast oscillations that are not observable on this time scale.

system is accurately given by

$$N_{\text{tot}} \approx \langle a_c^\dagger a_c \rangle e^{-2\gamma t} \{1 + [\text{Im}(\tilde{\zeta}_1 t)]^2\}, \quad (34)$$

where the  $\gamma$  is the decay constant associated with an individual cavity and the term involving  $\text{Im}(\tilde{\zeta}_1 t)$  is the correction term which arises due to the averaging of the losses over all the possible Bloch states. As mentioned earlier and as can be seen in Fig. 3, different Bloch states experience different losses, which explicitly indicates that assuming the same loss factor for every mode is not valid for CROW structures such as this. Thus, an important conclusion of our results is that due to the strong variation in loss for different Bloch modes, one should not expect exponential decay in the photon number in a CROW for a general initial state. We examine this effect more carefully shortly, but first turn to an examination of the quadrature variances and correlations.

Following a procedure similar to that used to arrive at Eq. (30), one can derive the following expressions for the variances of the quadrature operators in the CROW structure:

$$\begin{aligned} \langle (\Delta X_p)^2 \rangle &= 1 + 2 \langle a_c^\dagger a_c \rangle e^{-2\gamma t} |J_{\delta p}(\tilde{\zeta}_1 t)|^2 \\ &\quad + \langle a_c a_c \rangle e^{i\delta p \pi} J_{\delta p}^2(\tilde{\zeta}_1 t) e^{-2i\tilde{\Omega}_0 t} \\ &\quad + \langle a_c^\dagger a_c^\dagger \rangle e^{-i\delta p \pi} J_{\delta p}^2(\tilde{\zeta}_1^* t) e^{2i\tilde{\Omega}_0^* t} \end{aligned} \quad (35)$$

and

$$\begin{aligned} \langle (\Delta Y_p)^2 \rangle &= 1 + 2 \langle a_c^\dagger a_c \rangle e^{-2\gamma t} |J_{\delta p}(\tilde{\zeta}_1 t)|^2 \\ &\quad - \langle a_c a_c \rangle e^{i\delta p \pi} J_{\delta p}^2(\tilde{\zeta}_1 t) e^{-2i\tilde{\Omega}_0 t} \\ &\quad - \langle a_c^\dagger a_c^\dagger \rangle e^{-i\delta p \pi} J_{\delta p}^2(\tilde{\zeta}_1^* t) e^{2i\tilde{\Omega}_0^* t}. \end{aligned} \quad (36)$$

The time-dependent quadrature noise in  $X$  for lossy and lossless systems is shown in orange and gray, respectively, in Fig. 5 for different cavities in the CROW structure. As can be seen in Fig. 5(a), due to the nature of SVSSs, the quadrature noise in  $X$  is initially less than the classical limit (dashed line), as

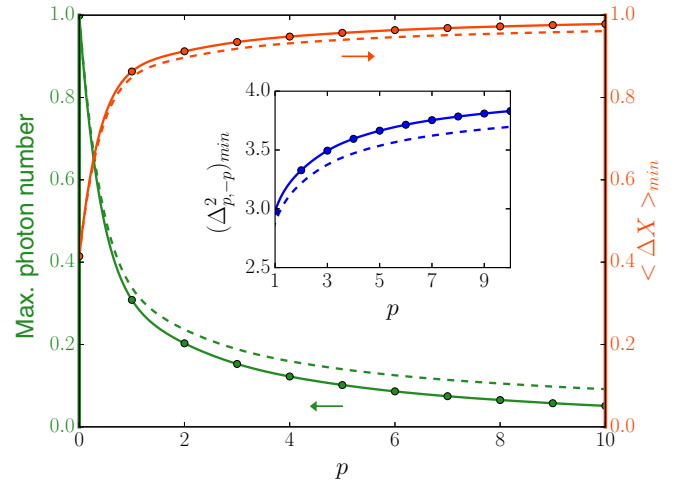


FIG. 6. Maximum number of photons (left axis) and minimum quadrature noise in  $X$  (right axis) in the first 11 cavities of the CROW. The inset shows the minimum correlation variance between different symmetrically displaced pairs of cavities. The dashed lines show the same quantities when the system is lossless.

expected. The coupling between the cavities and the scattering loss in the system degrades the squeezing in the cavities as the system evolves in time.

The maximum number of photons and the maximum squeezing in each cavity are shown in Fig. 6. As expected, both the maximum number of photons and squeezing in the  $X$  quadrature decrease as we move away from the central cavity. This is most evident when comparing the corresponding quantities for the tenth and the central cavities. The quadrature noise in  $X$  and the maximum photon number in the tenth cavity are 2.4 and 0.05 times the corresponding values at the zeroth cavity, respectively. This figure also shows the effects of loss on the maximum number of photons and maximum squeezing by comparing the lossy (solid line) and lossless (dashed line) results. As can be seen, in the absence of loss, the maximum number of photons is higher, as expected, and the quadrature noise in  $X$  is more squeezed, which is in agreement with our previous results on squeezed state generation in a single lossy cavity [26].

We now examine the effects of loss in more detail by returning to the results for photon number. Using Eq. (28), one can calculate the ratio  $R_p$  of the maximum photon number in the  $p$ th cavity in a lossy system to that in an idealized lossless system as a function of  $p$ . In Fig. 7(a), we plot the difference  $\Delta R_p$  between the exact  $R_p$  and what one would obtain using only the single-cavity exponential loss, i.e., assuming that  $\tilde{\beta}_1$  is real (dashed blue line). In the same figure, we also plot the difference between the exact  $R_p$  and an exponential fit to the loss (black line). As can be seen, both approximate results agree quite well with our results, with the maximum deviation being only about 0.01 for the selected range of  $p$ . This good agreement arises because the peaks in the photon number in each cavity are dominated by the Bloch modes for the photons with the maximum group velocity, which according to Fig. 3 are the modes close to  $k = \pi/2D$  with the corresponding quality factor close to  $Q_0$ . Now, to show that an exponential is not a good fit for all quantities, in Fig. 7(b), we plot the difference

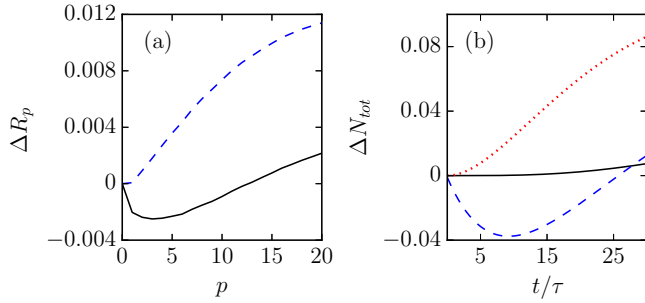


FIG. 7. Calculated results for the photon numbers in the CROW structure. (a) The deviation of the maximum photon number ratio from the pure exponential term in Eq. (28) (dashed blue line) and from an exponential fit (black line),  $e^{-at}$ , where  $a = 1.5 \times 10^{-4}$  as a function of  $p$ . (b) The deviation of the total photon number from the exact result of Eq. (33) for (1) Eq. (34) (solid black line), (2) a pure exponential factor in Eq. (33) (dotted red line), and (3) an exponential fit (dashed blue line) with fitting parameter  $a = 3.8 \times 10^{-4}$ .

$\Delta N_{\text{tot}}$  between the results from Eq. (33) and (1) Eq. (34) (solid black line), (2) the pure exponential term in Eq. (33) (dotted red line), and (3) an exponential fit (dashed blue line). As can be seen, a purely exponential fit does not agree well with our results. This is due to the fact that our initial condition results in a state that has equal weight in all of the Bloch modes and therefore includes modes that have a wide range of group velocities and quality factors. This shows that one cannot necessarily assume a simple exponential decay when treating CROW structures or any other coupled-cavity structures if the coupled modes have significantly different quality factors. The degree of deviation from pure exponential decay will depend on the structure and the initial state of the system.

We now study the inseparability criteria for the squeezed light inside the CROW structure. Using Eqs. (13), the time-dependent correlation variance can be written as

$$\begin{aligned} \Delta_{p,p'}^2 = & 4 + 4 \langle a_c^\dagger a_c \rangle e^{-2\gamma t} [ |J_{\delta p}(\tilde{\zeta}_1 t)|^2 + |J_{\delta p'}(\tilde{\zeta}_1 t)|^2 ] \\ & - 4 \langle a_c a_c \rangle e^{-2i\tilde{\Omega}_0 t} e^{i(\delta p + \delta p')\pi/2} J_{\delta p}(\tilde{\zeta}_1 t) J_{\delta p'}(\tilde{\zeta}_1 t) \\ & - 4 \langle a_c^\dagger a_c^\dagger \rangle e^{2i\tilde{\Omega}_0^* t} e^{-i(\delta p + \delta p')\pi/2} J_{\delta p}(\tilde{\zeta}_1^* t) J_{\delta p'}(\tilde{\zeta}_1^* t), \end{aligned} \quad (37)$$

where the sum of the last three terms needs to be negative for the inseparability criteria for the CVs to be fulfilled.

In Fig. 8, we plot the time-dependent correlation variances for different sets of lossy and lossless cavities in blue and gray, respectively. The dashed lines show the inseparability criteria below which the light is considered to be entangled. Here we only focus on cases where the two cavities considered are located the same distance from the central cavity, as this will yield the maximum entanglement; however, using Eq. (37) one can explore the entanglement between any two cavities of the CROW. As can be seen, the maximum entanglement between each pair of cavities occurs when the peak in the photon number arrives at those cavities. Indeed, as time passes and the system evolves in time, the photons either scatter to the environment or move along the CROW, leading to a reduction in the number of photons in the considered cavity and consequently a decrease in the degree of entanglement. In

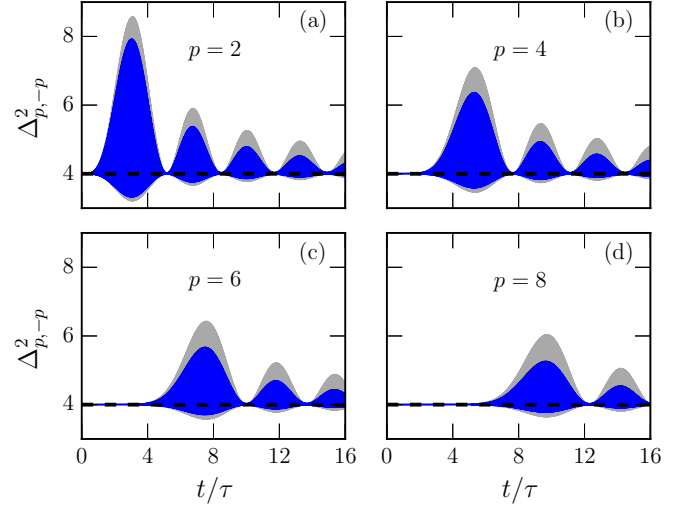


FIG. 8. Correlation variance between different pairs of cavities in the CROW as a function of time. The results for a lossless system are shown in light gray.

order to compare the entanglement between different sets of cavities, in the inset to Fig. 6 we plot the minimum correlation variance as a function of cavity index,  $p$ . The dashed lines show the results when the effects of loss are ignored. As expected, the difference between the lossy and the ideal systems is more evident as we get away from the central cavity.

Finally, in order to provide better insight into how the maximum number of photons, the minimum quadrature noise in  $X$ , and the minimum correlation variance vary with cavity number in a *lossless* CROW system for the cavities far from the central cavity (large  $p$ ) when the  $c = 0$  cavity is initially in the SVS, we use asymptotic expansion expressions for the Bessel functions [44] in Eqs. (30), (35), and (37) to obtain

$$\langle a_p^\dagger a_p \rangle_{\text{max}} \approx \frac{c_1^2 \sinh^2(u)}{p^{2/3}}, \quad (38)$$

$$\langle (\Delta X_p)^2 \rangle_{\text{max}} \approx 1 - \frac{c_1^2 (1 - e^{-2u})}{p^{2/3}}, \quad (39)$$

and

$$(\Delta_{p,-p}^2)_{\text{max}} \approx 4 \left[ 1 - \frac{c_1^2 (1 - e^{-2u})}{p^{2/3}} \right], \quad (40)$$

where  $c_1 = 2^{1/3} \text{Ai}(-2^{1/3} c_0) \approx 0.67$ , where Ai is the Airy function. It can be seen that for all three quantities, the dependence on  $p$  is  $p^{2/3}$ .

## V. CONCLUSION

In this work, we have examined the time evolution of squeezed states in coupled-cavity systems. We have applied the tight-binding method to evaluate the fields and complex frequencies for the leaky modes of lossy coupled-cavity system.

We have presented the analytic time-dependent expressions for the photon number, quadrature noise, and correlation variance in the simple two-coupled-cavity system and in a lossy CROW structure in terms of Bessel functions.



We have examined how the nonclassical properties of light in one cavity will be transferred to the other cavities in lossy coupled-cavity systems and have shown how loss affects properties such as photon number, quadrature squeezing, and entanglement. Moreover, we have studied the maximum values of these three quantities in both a lossy and a lossless system and have derived approximate analytic expressions for the  $p$  dependence of the maximum values of these three quantities in the absence of loss.

Our analytic results enabled the investigation of the effects of loss for any CROW structure that can be modeled using the nearest-neighbor tight-binding approximation. The importance of loss depends on the initial conditions as well as the single-cavity loss, the group velocity, and the loss dispersion of the particular CROW being studied. We have found that for the CROW structure considered in this work, the effects of loss are significant and should not be neglected. In particular, we have shown that when the Bloch modes have very different quality factors, the effects of loss cannot generally be treated by using a simple exponential loss factor.

Although we have focused on the squeezed states in this work, one can study the same quantities of the other states of light such as squeezed thermal states and coherent states by simply replacing the corresponding quantities in the expressions provided in this paper.

Finally, it should be mentioned that here, rather than employing a continuous-wave pump to generate nonclassical light in the central cavity, we have focused on the time evolution of an initially generated squeezed state in the system. The full process of generation and evolution of the squeezed state in a coupled-cavity system and evaluating the dynamics of continuous-variable entanglement in such a system under continuous-wave pumping will be explored in future work.

#### ACKNOWLEDGMENTS

This work was supported by Queen's University and the Natural Sciences and Engineering Research Council of Canada (NSERC). The authors would also like to gratefully thank John E. Sipe and Mohsen Kamandar Dezfouli for many fruitful discussions.

- 
- [1] N. Cerf, N. Cerf, G. Leuchs, and E. Polzik, *Quantum Information with Continuous Variables of Atoms and Light* (Imperial College Press, London, 2007).
  - [2] D. Bouwmeester, A. Ekert, and A. Zeilinger, *The Physics of Quantum Information: Quantum Cryptography, Quantum Teleportation, Quantum Computation* (Springer, Berlin, 2013).
  - [3] D. Huang, P. Huang, D. Lin, and G. Zeng, *Sci. Rep.* **6**, 19201 (2016).
  - [4] A. Leverrier and P. Grangier, *Phys. Rev. A* **83**, 042312 (2011).
  - [5] D. B. S. Soh, C. Brif, P. J. Coles, N. Lütkenhaus, R. M. Camacho, J. Urayama, and M. Sarovar, *Phys. Rev. X* **5**, 041010 (2015).
  - [6] X. Jia, X. Su, Q. Pan, J. Gao, C. Xie, and K. Peng, *Phys. Rev. Lett.* **93**, 250503 (2004).
  - [7] Y. Miwa, J.-I. Yoshikawa, P. van Loock, and A. Furusawa, *Phys. Rev. A* **80**, 050303(R) (2009).
  - [8] P. van Loock and S. L. Braunstein, *Phys. Rev. Lett.* **84**, 3482 (2000).
  - [9] S. L. Braunstein and P. van Loock, *Rev. Mod. Phys.* **77**, 513 (2005).
  - [10] L.-M. Duan, G. Giedke, J. I. Cirac, and P. Zoller, *Phys. Rev. Lett.* **84**, 2722 (2000).
  - [11] R. Simon, *Phys. Rev. Lett.* **84**, 2726 (2000).
  - [12] A. M. Marino, R. C. Pooser, V. Boyer, and P. D. Lett, *Nature (London)* **457**, 859 (2009).
  - [13] G.-X. Li, H.-T. Tan, and M. Macovei, *Phys. Rev. A* **76**, 053827 (2007).
  - [14] S. Pielawa, G. Morigi, D. Vitali, and L. Davidovich, *Phys. Rev. Lett.* **98**, 240401 (2007).
  - [15] G. Masada, K. Miyata, A. Politi, T. Hashimoto, J. L. O'Brien, and A. Furusawa, *Nat. Photon.* **9**, 316 (2015).
  - [16] A. Rai and D. G. Angelakis, *Phys. Rev. A* **85**, 052330 (2012).
  - [17] A. B. U'Ren, R. K. Erdmann, M. de la Cruz-Gutierrez, and I. A. Walmsley, *Phys. Rev. Lett.* **97**, 223602 (2006).
  - [18] L. Sciscione, M. Centini, C. Sibilìa, M. Bertolotti, and M. Scalora, *Phys. Rev. A* **74**, 013815 (2006).
  - [19] Z. Yang and J. E. Sipe, *Opt. Lett.* **32**, 3296 (2007).
  - [20] A. Fiore, V. Berger, E. Rosencher, P. Bravetti, and J. Nagle, *Nature (London)* **391**, 463 (1998).
  - [21] L. Lanco, S. Ducci, J.-P. Likforman, X. Marcadet, J. A. W. van Houwelingen, H. Zbinden, G. Leo, and V. Berger, *Phys. Rev. Lett.* **97**, 173901 (2006).
  - [22] A. Orioux, X. Caillet, A. Lemaître, P. Filloux, I. Favero, G. Leo, and S. Ducci, *J. Opt. Soc. Am. B* **28**, 45 (2011).
  - [23] A. Yariv, Y. Xu, R. K. Lee, and A. Scherer, *Opt. Lett.* **24**, 711 (1999).
  - [24] N. Ashcroft and N. Mermin, *Solid State Physics* (Cengage Learning, Boston, MA, 2011).
  - [25] D. P. Fussell and M. M. Dignam, *Appl. Phys. Lett.* **90**, 183121 (2007).
  - [26] H. Seifoori, S. Doutre, M. M. Dignam, and J. E. Sipe, *J. Opt. Soc. Am. B* **34**, 1587 (2017).
  - [27] H.-T. Tan, W.-M. Zhang, and G.-x. Li, *Phys. Rev. A* **83**, 062310 (2011).
  - [28] H.-N. Xiong, W.-M. Zhang, X. Wang, and M.-H. Wu, *Phys. Rev. A* **82**, 012105 (2010).
  - [29] H.-T. Tan and W.-M. Zhang, *Phys. Rev. A* **83**, 032102 (2011).
  - [30] D. P. Fussell and M. M. Dignam, *Phys. Rev. A* **77**, 053805 (2008).
  - [31] M. K. Dezfouli and M. M. Dignam, *AIP Adv.* **4**, 123003 (2014).
  - [32] H. P. Breuer and F. Petruccione, *The Theory of Open Quantum Systems* (Oxford University Press, Oxford, 2007).
  - [33] M. M. Dignam and M. K. Dezfouli, *Phys. Rev. A* **85**, 013809 (2012).
  - [34] H. Zoubi, M. Orenstien, and A. Ron, *Phys. Rev. A* **62**, 033801 (2000).
  - [35] A. Rai, G. S. Agarwal, and J. H. H. Perk, *Phys. Rev. A* **78**, 042304 (2008).
  - [36] E. Ozbay, M. Bayindir, I. Bulu, and E. Cubukcu, *IEEE J. Quantum Electron.* **38**, 837 (2002).

- [37] T. Kamalakis and T. Sphicopoulos, *IEEE J. Quantum Electron.* **41**, 1419 (2005).
- [38] Y. Zhang, R. Okubo, M. Hirano, Y. Eto, and T. Hirano, *Sci. Rep.* **5**, 13029 (2015).
- [39] M. Kamandar Dezfouli, Ph.D. thesis, Queen's University, 2015.
- [40] D. P. Fussell and M. M. Dignam, *Opt. Lett.* **32**, 1527 (2007).
- [41] L.-A. Wu, H. J. Kimble, J. L. Hall, and H. Wu, *Phys. Rev. Lett.* **57**, 2520 (1986).
- [42] C. Gerry and P. Knight, *Introductory Quantum Optics* (Cambridge University Press, Cambridge, 2004).
- [43] F. W. Olver, D. W. Lozier, R. F. Boisvert, and C. W. Clark, *NIST Handbook of Mathematical Functions*, 1st ed. (Cambridge University Press, New York, 2010).
- [44] M. Abramowitz, *Handbook of Mathematical Functions, With Formulas, Graphs, and Mathematical Tables* (Dover, New York, 1974).